Supporting Information

Rotisserie-like Motion Enables Guest Transport in a Nonporous Organic Crystal Involving a Diboron Host

Gonzalo Campillo-Alvarado,[a,] Eva C. Vargas-Olvera,[b] Dale C. Swenson,[c] Hugo Morales-Rojas,[b] Herbert Höpfl[b] and Leonard R. MacGillivray[c,d,*]*

[a]*Department of Chemistry, Reed College, Portland, OR 97202-8199, United States.*

[b]*Centro de Investigaciones Químicas, Instituto de Investigación en Ciencias Básicas y Aplicadas, Universidad Autónoma del Estado de Morelos, Av. Universidad 1001, Cuernavaca, 62209, México*

[c]*Department of Chemistry, University of Iowa, Iowa City, Iowa 52242, United States*

[d]*Département de Chimie, Université de Sherbrooke, Sherbrooke, QC, J1K 2R1 Canada*

E-mail: leonard.macgillivray@usherbrooke.ca
gcampillo@reed.edu

S1. Supplemental Experimental Procedures

Materials:

2,4-difluorophenylboronic acid, catechol, 4,4'-azopyridine (**4,4'-apy**) and benzene were obtained from Sigma Aldrich and used without further purification. Difluorophenylboronic acid catechol ester (**1**) was synthesized following a reported literature procedure.[1]

Synthesis of **S**: **1** (0.050 g, 0.216 mmol) and **4,4'-apy** (0.020 g, 0.108 mmol) were dissolved in 2.5 mL of benzene). The solution was gently heated in a sealed vial until the starting materials were completely dissolved. Crystals of **S** in the form of dark-red prisms formed upon slow evaporation of the solution at room temperature after 3 days. The crystallization vial contained traces (1:10) of single crystals of **I** in the form of red prisms.

Synthesis of **D**: Single crystals of **S** transform into **D** spontaneously under ambient temperature and pressure after ca. 1.5 hours after being removed from the mother liquor in the crystallization vial.

Instruments and methods:

Single-crystal X-ray diffraction data for **S** and **D** were collected on a Nonius Kappa CCD single-crystal X-ray diffractometer using MoKα radiation (λ=0.71073 Å). Data for **I** were collected on a Bruker Nonius APEX II Kappa single-crystal X-ray diffractometer using MoKα radiation (λ=0.71073 Å) graphite monochromator equipped with an Oxford Cryostream low temperature device. Crystals were mounted in Paratone oil on a Mitegen magnetic mount. Lorentz and polarization corrections were applied and programs from the APEXII package were used for data reduction. Structure solution and refinement were accomplished using SHELXL[2] and SHELXT,[3] respectively within the Olex2[4] graphical user interface. Non-hydrogen atoms were refined anisotropically and hydrogen atoms were placed in geometrically calculated positions using a riding model. Crystal structures were generated using Mercury, Olex2 and Diamond software packages. Metrics were calculated using Olex2 from the .res files using shelxl matrices.

Thermogravimetric and differential scanning calorimetry (TG-DSC) analyses were performed on a TA SDT Q600 instrument with approximately 3.5 mg of a crystalline solid sample at a heating rate of 10°C/min within the temperature range of 30−600°C using a current of nitrogen as inert gas purge (50 mL/min). Scans were analyzed with Universal V4.2E TA Instruments software package. ^{1}H NMR spectra were recorded on a Bruker Ascend Evo 400 MHz spectrometer with chloroform-d as internal standard.

Theoretical studies based on density functional theory (DFT) were used to explore the molecular geometry and energy of the systems. All calculations were carried out using the Gaussian16 program using the 6-311 + + G(d,p) basis set.[5] Molecular coordinates were obtained from the SCXRD data. Geometry optimizations of single crystal structures were performed by fixing non-hydrogen atom coordinates, and only hydrogen atoms were optimized. Fully geometry optimized structures of **S** and **I** without benzene were calculated for comparison.

S2. Single-crystal X-ray Diffraction Data

Table S1. Crystallographic parameters for **S**, **D** and **I**.

Compound name	**S**	**D**	**I**
Empirical formula	$C_{34}H_{22}B_2F_4N_2O_4 \supset 2C_6H_6$	$C_{34}H_{22}B_2F_4N_2O_4$	$C_{34}H_{22}B_2F_4N_2O_4 \supset C_6H_6$
Formula weight	804.42	648.19	726.30
Temperature/K	298.15	298.15	190.15
Crystal system	monoclinic	monoclinic	monoclinic
Space group	$P2_1/c$	$P2_1/n$	$P2_1/c$
a/Å	7.5341(8)	7.3611(12)	12.6124(13)
b/Å	14.4259(14)	13.623(2)	15.3927(15)
c/Å	16.8748(17)	15.855(3)	17.4936(17)
α/°	90	90	90
β/°	92.484(5)	102.723(11)	105.945(5)
γ/°	90	90	90
Volume/Å^3	1832.3(3)	1550.9(5)	3265.5(6)
Z	2	2	4
ρ_{calc}g/cm^3	1.316	1.388	1.398
μ/mm^{-1}	0.099	0.107	0.106
F(000)	748.0	664.0	1412.0
Crystal size/mm^3	0.34 × 0.16 × 0.12	0.34 × 0.16 × 0.12	0.19 × 0.13 × 0.08
Radiation	MoKα (λ = 0.71073)	MoKα (λ = 0.71073)	MoKα (λ = 0.71073)
2Θ range for data collection/°	5.648 to 47.998	5.268 to 48.996	5.35 to 52.82
Index ranges	-7 ≤ h ≤ 8, -16 ≤ k ≤ 16, -19 ≤ l ≤ 19	-8 ≤ h ≤ 7, -13 ≤ k ≤ 15, -18 ≤ l ≤ 18	-15 ≤ h ≤ 15, -18 ≤ k ≤ 18, -21 ≤ l ≤ 21
Reflections collected	8676	8293	35911
Independent reflections	2823 [R_{int} = 0.1190, R_{sigma} = 0.1185]	2587 [R_{int} = 0.1074, R_{sigma} = 0.1087]	6620 [R_{int} = 0.0594, R_{sigma} = 0.0606]
Data/restraints/parameters	2823/36/260	2587/0/209	6620/511/475
Goodness-of-fit on F^2	0.954	0.999	1.030
Final R indexes [I>=2σ (I)]	R_1 = 0.0660, wR_2 = 0.1601	R_1 = 0.0809, wR_2 = 0.1551	R_1 = 0.0719, wR_2 = 0.1799
Final R indexes [all data]	R_1 = 0.1749, wR_2 = 0.2100	R_1 = 0.2115, wR_2 = 0.1857	R_1 = 0.1303, wR_2 = 0.2171
Largest diff. peak/hole / eÅ^{-3}	0.43/-0.22	0.18/-0.19	0.56/-0.43
CCDC deposition number	1998621	1998622	1998623

Table S2. Hydrogen bond and π···π contact parameters for **S**, **D** and **I**.

Crystal	D–H···A/ Centroid···Centroid	*d*(D–H) [Å]	*d*(H···A) [Å]	*d*(D···A) [Å]	∠(D–H···A) [deg]	Symmetry code
S	C17–H17···F2	0.930	2.486	3.398	166.7	-x,-1/2+y,1/2-z
	C13–H13···F1	0.930	2.504	3.272	140.2	-
	Cg1···Cg2[1]	-	-	3.898	-	-
D	C13–H13···F2	0.930	2.465	3.346	158.2	-x+1/2, y+1/2, -z+3/2
	Cg1···Cg2[2]	-	-	3.771	-	-x+3/2, y-1/2, -z+3/2
I	C25–H25···F3	0.950	2.544	3.328	134.0	-x, y+1/2, -z+3/2
	Cg1···Cg2[3]	-	-	3.676	-	-x+1,y-1/2,-z+3/2
	Cg3···Cg4[3]	-	-	3.877	-	-x+1,y-1/2,-z+3/2
	Cg5···Cg6[3]	-	-	3.737	-	-x,y+1/2,-z+3/2

[1]Cg1 = N1, C13–C17; Cg2 = C18–C23. [2]Cg1 = C1–C6; Cg2 = N1, C13–C17. [3]Cg1 = C1–C6; Cg2 = N1, C13–C17; Cg3 = C7–C12; Cg4 = N4, C18–C22; Cg5 = C23–C28; Cg5 = C29–C34; Cg6 = N1, C13–C17.

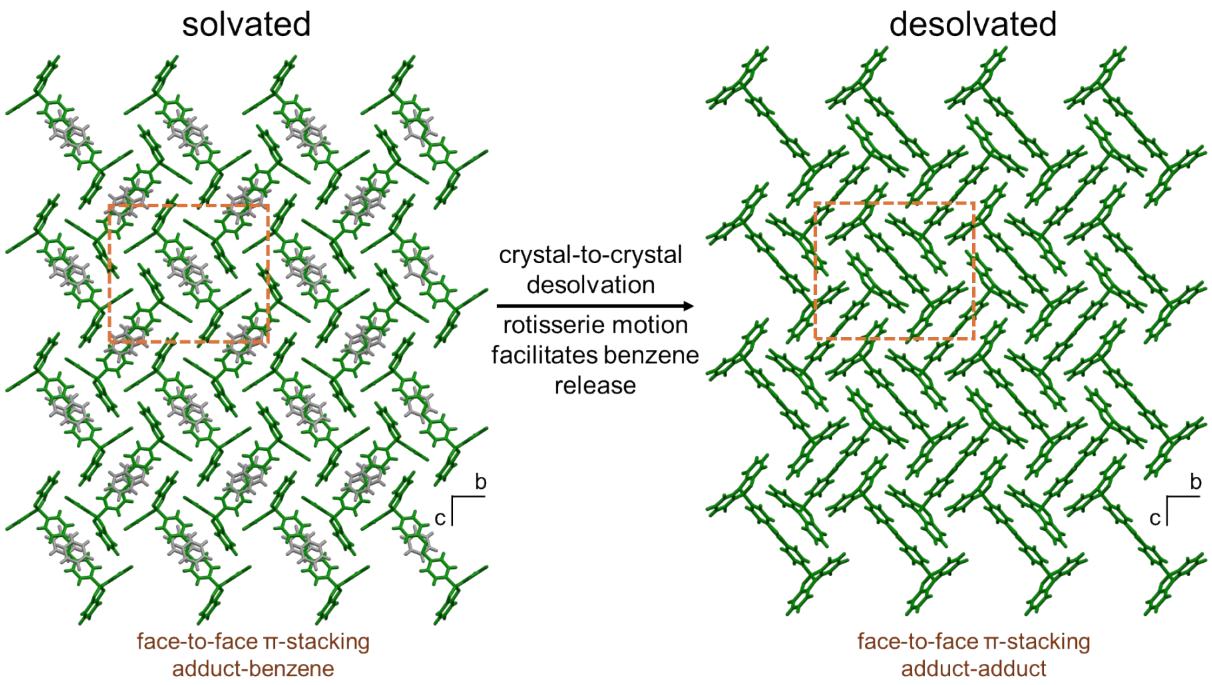

Figure S1. Crystal structures of **S** (left) and **D** (right) depicting the observed cooperative rotisserie-like motion that facilitates crystal-to-crystal desolvation. In the **S** crystal, adduct-benzene is primarily supported by face-to-face π-stacking whereas rotisserie-like rotation of azopyridine in **D** generates face-to-face π-stacking between adjacent adducts.

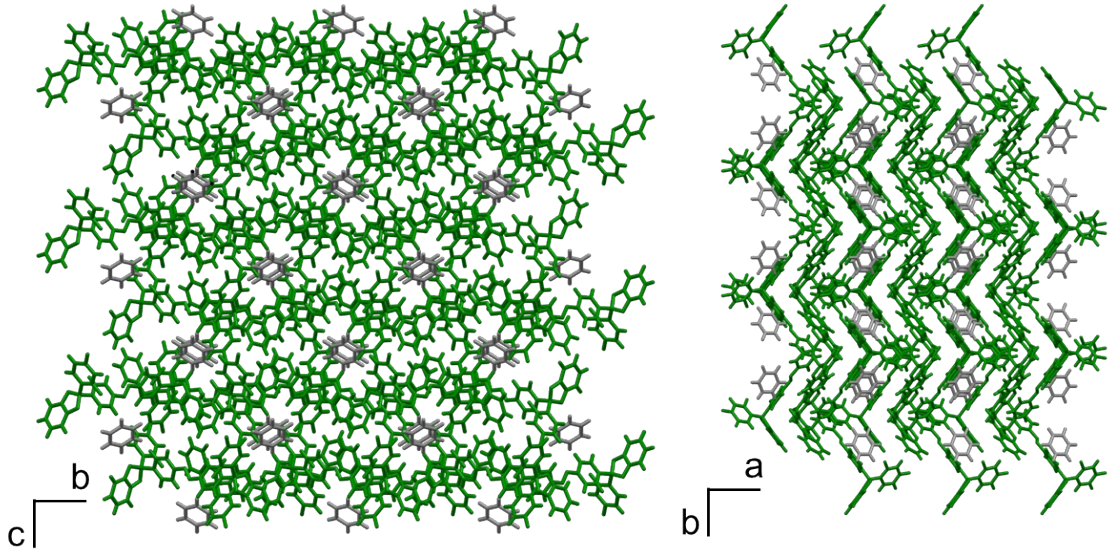

Figure S2. Crystal structure view of **I**, showing the inclusion of benzene molecules via edge-to-face π-stacking. The packing of adducts shows close face-to-face π-stacking, directing the benzene molecule to the generated side cavities of the assembly.

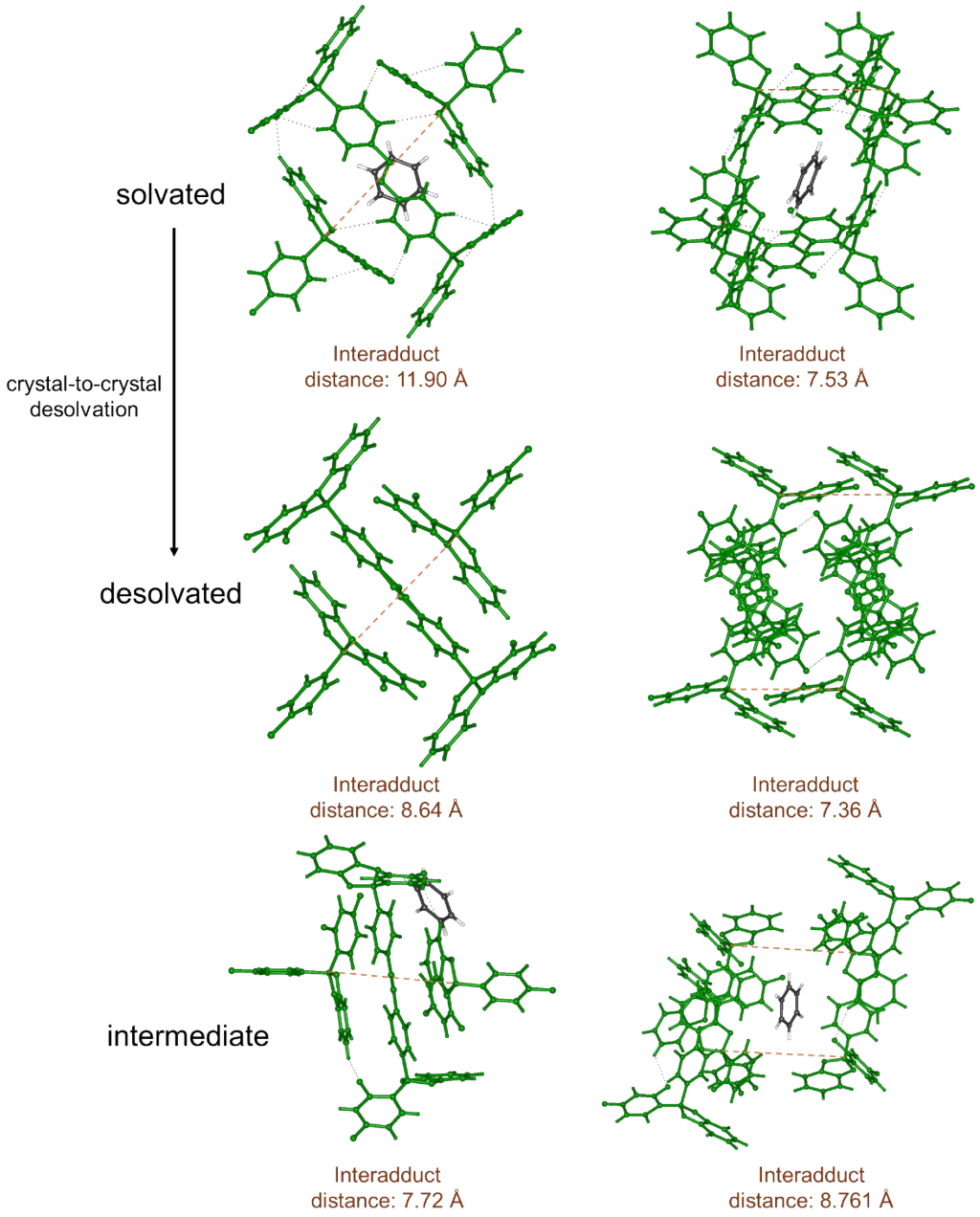

Figure S3. Crystal structures of solvated, **S** (top), desolvated, **D** (middle), and intermediate, **I** (bottom). The structures of **S** and **D** show the changes in interadduct distances upon desolvation in two different views. Upon a rotisserie-style conformational change and desolvation, the adducts approach one another, maximizing face-to-face π-stacking. The crystal structure of **I** shows the presence of face-to-face π-stacking and the placement of benzene on the side of the assembly by face-to-face π-stacking.

S3. Thermal data

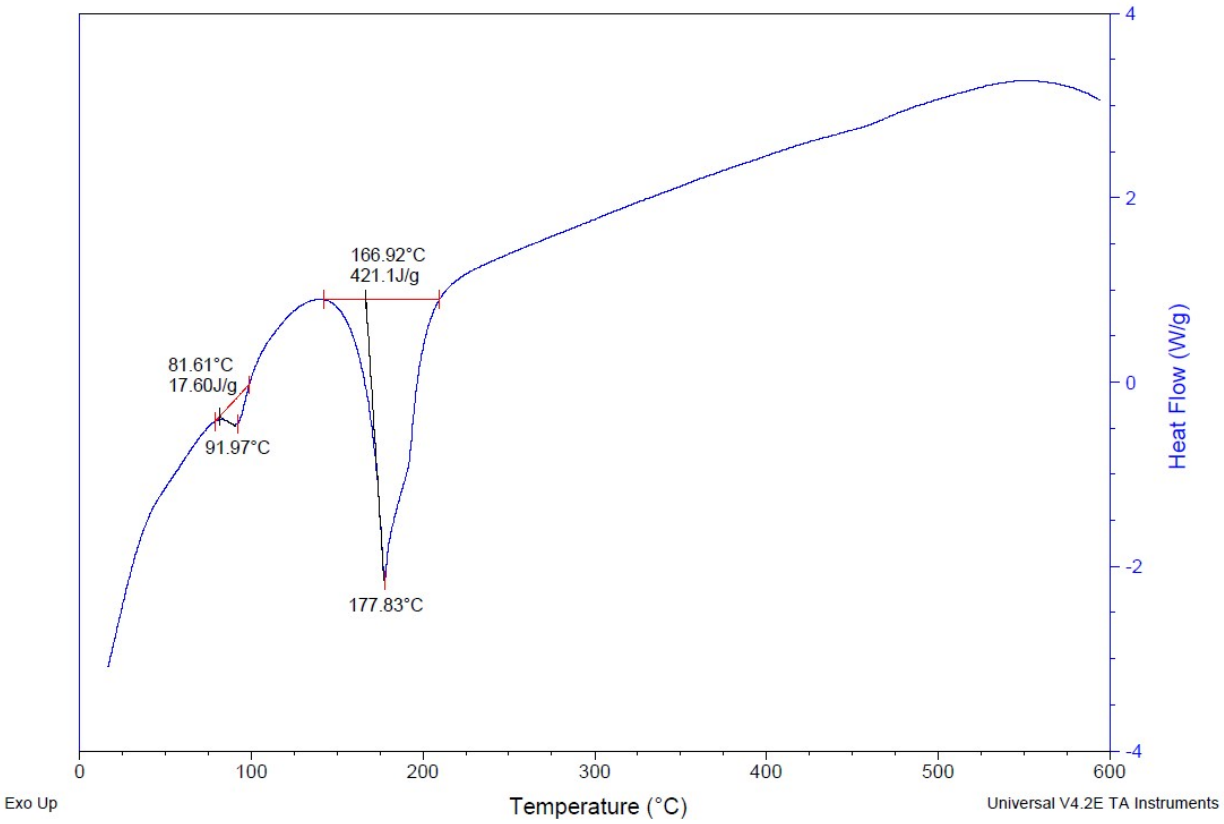

Figure S4. Differential scanning calorimetry analysis of **S**.

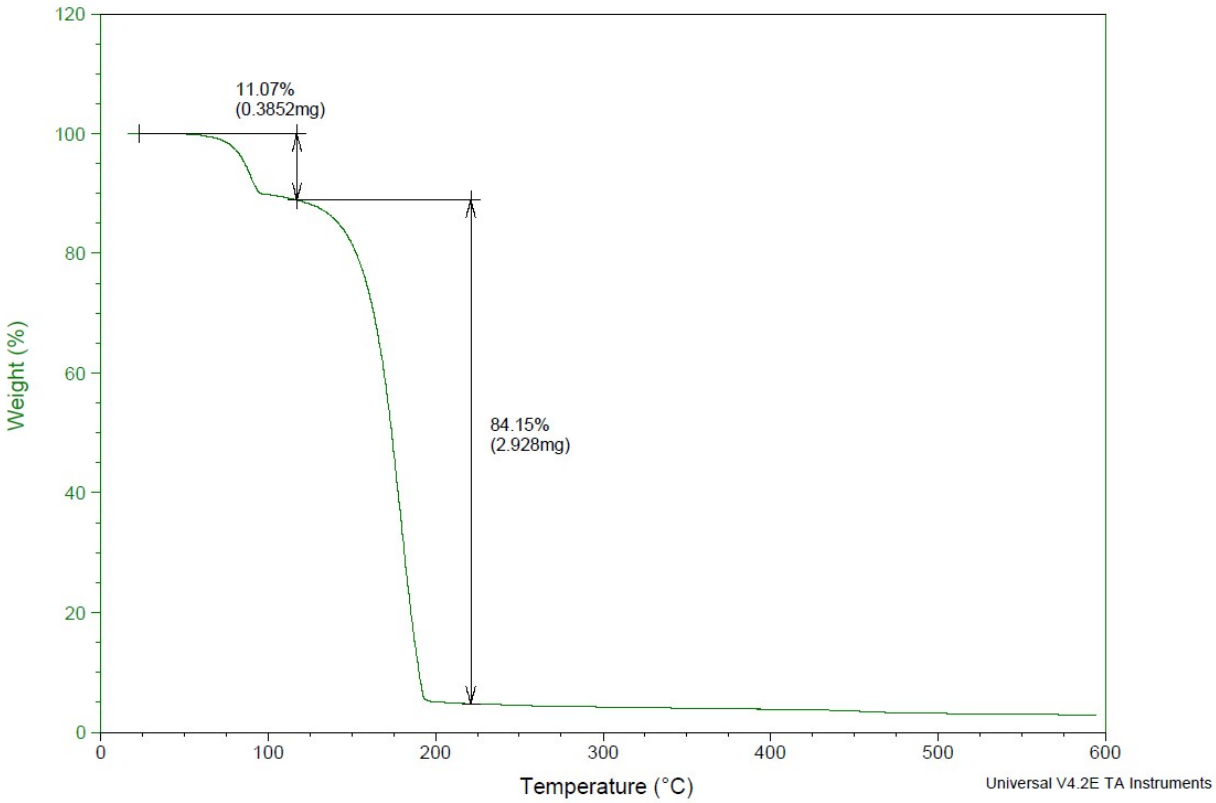

Figure S5. Thermogravimetric analysis of **S**.

S4. Molecular modeling data

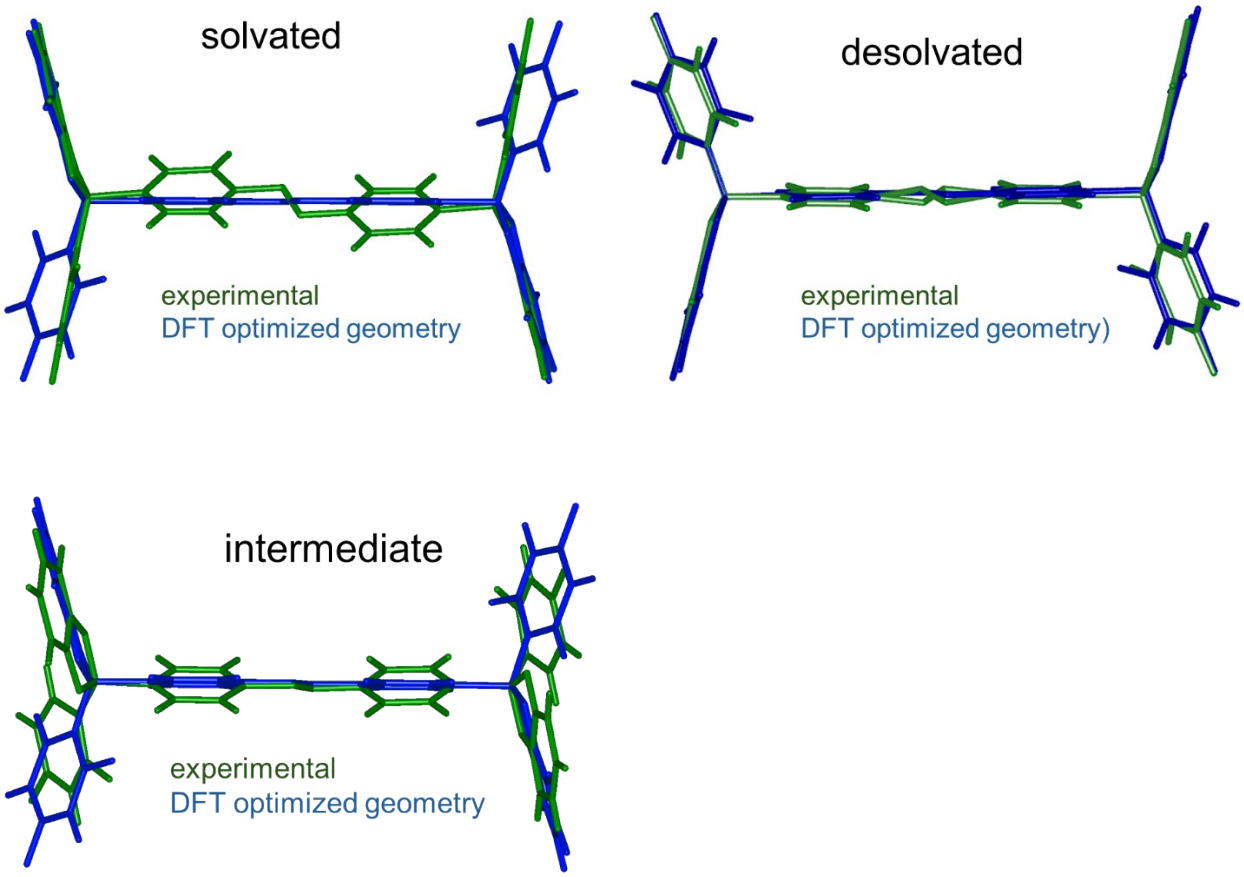

Figure S6. Overlays of molecular conformations of crystal structures of solvated (**S**), desolvated (**D**), and intermediate (**I**) structures (green), and their resulting conformations after geometry optimization (blue).

S4. Molecular modeling data

Table S3. Calculated electronic energies (E_{SFC}, Hartree) and relative energies (ΔE, kcal/mol) for diboron adducts **S** and **I** before and after geometry optimization.

System	**E_{SFC} (Hartree)**	**ΔE (kcal/mol)**
S	-2278.579703	0 (reference)
S, geometry optimized	-2278.611382	-19.878877
I	-2278.599827	0 (reference)
I, geometry optimized	-2278.611596	-7.385161

S5. ^{1}H nuclear magnetic resonance data

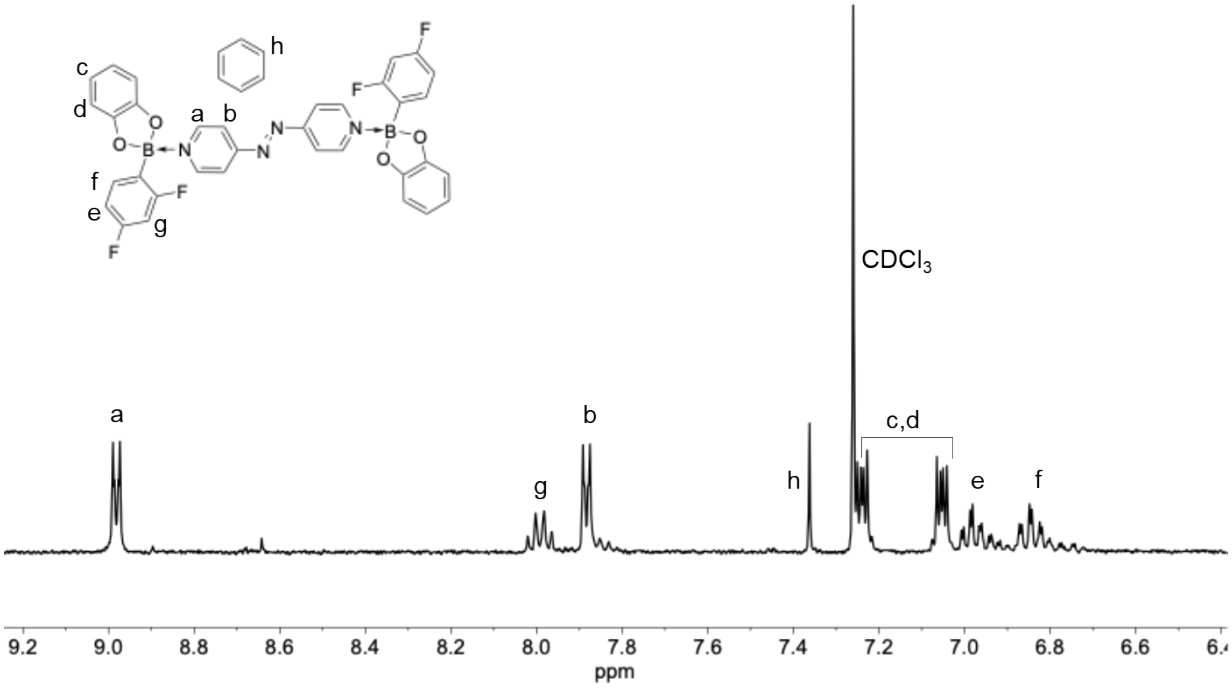

Figure S7. ^{1}H NMR spectrum of **S**.

S4. Supplemental References

1. G. Campillo-Alvarado, E. C. Vargas-Olvera, H. Höpfl, A. D. Herrera-España, O. Sánchez-Guadarrama, H. Morales-Rojas, L. R. MacGillivray, B. Rodríguez-Molina and N. Farfán, *Cryst. Growth Des.*, 2018, **18**, 2726-2743.
2. G. M. Sheldrick, *Acta Cryst. C*, 2015, **71**, 3-8.
3. G. M. Sheldrick, *Acta Cryst. A*, 2015, **71**, 3-8.
4. O. V. Dolomanov, L. J. Bourhis, R. J. Gildea, J. A. Howard and H. Puschmann, *J. Appl. Crystallogr.*, 2009, **42**, 339-341.
5. Z. Zebbiche, G. Şekerci, B. Houssem, F. Küçükbay, S. Tekin, H. Küçükbay and B. Boumoud, *J. Biochem. Mol. Toxicol.*, 2025, **39**, e70346.